Projections of oil palm area in Malaysia and Indonesia to assess the relationship between plant growth and water consumption

Chihiro Naito[1,2], Wataru Takeuchi[2]
[1] The Graduate School of Engineering, the University of Tokyo, Meguro-ku, Tokyo, Japan - chihiro-naito807@g.ecc.u-tokyo.ac.jp
[2] Institute of Industrial Sciences, the University of Tokyo, Meguro-ku, Tokyo, Japan - wataru@iis.u-tokyo.ac.jp

Keywords: Solar-induced fluorescence (SIF), El Niño, Precipitation, Vulnerability, Principal component analysis

Abstract

Palm oil is a widely used agricultural crop in the world, and most of them are produced in Malaysia and Indonesia covering millions of hectares. However, climate change which induces water stress and extreme weather such as El Niño poses a risk to oil palm production. Therefore, it is crucial to identify areas vulnerable to climate change to prioritize adaptation actions for sustainable palm oil production. Several studies have implemented vulnerability assessments for climate change using a limited number of climate variables, despite the complex relationships among vegetation and various water components. Given these situations, this study aims to identify areas vulnerable to climate change for oil palms by analyzing the relationship between vegetation productivity and climate variables, and their changes from 2002 to 2012 and from 2013 to 2022. This analysis utilized satellite-based multiple water components and applied principal component analysis. The identified vulnerable areas were then compared with the biophysical suitability map from another study. Severe El Niño impacts from 2015 to 2016 were also assessed as an indicator of the actual decline in productivity. The results showed that more than half of the study area had experienced water stress recently, particularly in Java, southern Borneo, and the southern New Guinea islands. There was a discrepancy between the biophysical suitability map and the identified vulnerable areas in this study, especially in the southern part of Borneo. These findings highlighted the importance of considering multiple water components in tropical regions and future projections for appropriate palm oil cultivation areas.

1. Introduction

Palm oil is the most widely produced edible oil in the world. Malaysia and Indonesia are the dominant producers with millions of hectares for its cultivation. Global demand for palm oil is expected to rise due to population growth and increased industrial applications, including bioenergy usage. Despite this growing demand, palm oil production is projected to face negative impacts from climate change, particularly water stress (Fleiss, et al., 2017). Additionally, the available land for expanding cultivation is limited due to concerns about deforestation. To sustain and enhance productivity within these vast yet restricted areas, it is crucial to identify areas vulnerable to climate change to prioritize areas for adaptation strategies. Identifying non-vulnerable areas can help intensify productivity, while detecting vulnerable areas can facilitate the application of appropriate management practices, thereby preventing the exhaustion of environmental and operational resources.

Generally, oil palms prefer high temperatures, and balanced precipitation and soil evaporation an important factors for their growth (Corley and Tinker, 2015). Khiabani, et al. (2020) developed a biophysical suitable map for oil palms using five meteorological and two geomorphological criteria including temperature, precipitation, elevation, and slope based on the contexts of the framework proposed by Food and Agriculture Organization of the United Nations (FAO).

However, Climate change is projected to affect the climate environment in the primary palm oil-producing countries, Malaysia and Indonesia. A climate scenario suggests that the temperature could rise by 1.7 to 4.2 degrees Celsius across Malaysia, while precipitation will exhibit spatial and seasonal variance by the end of the 21st century (Loh et al., 2016). The extreme weather associated with El Niño is projected to become more frequent in Indonesia (Tangang et al., 2020). These impacts may be altering suitable conditions for oil palms.

To understand climate change impacts on vegetation, several studies have been conducted to capture the responses of vegetation to climate factors and disturbances. For example, Seddon et al. (2016) analyzed the relationships between climate variables and enhanced vegetation index (EVI) using satellite data on a global scale. These studies define high sensitivity as vulnerable to climate change or disturbances.
Regarding oil palms, Paterson et al. (2015) simulated changes in the suitable regions for oil palm cultivation using climate models, indicating most areas will remain suitable by 2070**.**
Many of these models or simulations, however, utilize a few climate parameters such as precipitation and temperature, or focus on a country-wide production despite the complexity of ecosystems. In addition, the magnitude of the influence of climate variables may vary among places. Therefore, assessing the spatial heterogeneity of impacts and the response of vegetation to climate variables is important. Tracking changes in these responses over different periods can help identify particularly sensitive areas to climate change.

Given the conditions mentioned above, this study aims to: (1) assess the vegetation responses and these changes to climate variables or disturbances at different periods to identify vulnerable areas for vegetation to water stress and (2) compare the identified vulnerable areas with the biophysical suitability map for oil palm cultivation. The analysis utilized satellite time series data.

2. Methodology

2.1 Study area

The study area of this research is the land area of Malaysia and Indonesia. Both countries are located in Southeast Asia, and classified as tropical regions based on the Köppen-Geiger climate classification.

2.2 Dataset

Satellite data used in this study included data on Solar Induced Chlorophyll Fluorescence (SIF) as an indicator of plant growth. The GOSIF dataset (Li and Xiao, 2019) was selected for its high spatial and temporal resolution (0.05°, 8-day). Water components as climate variables included Temperature at 2 meters above the surface from ERA5-Land hourly data from 1950 to the present (hereafter referred to as ERA5, 0.1°, daily), precipitation from GPM IMERG L3 (0.1°, daily), evaporation and transpiration, both from GLEAM v3.8a (0.25°, daily), and soil moisture and vegetation optical depth (VOD) at 6.9 GHz from AMSR-E/Aqua L2B V002 (from June 2002 to November 2011) and AMSR2/GCOM-W1 L3 (from November 2011 to December 2022). VPD was calculated based on Liu et al., 2024).

All data was resampled into a spatial resolution of 0.1°. The study period was set from January 2003 to December 2021, and this period was separated from 2002 to 2012 (the first period) and from 2013 to 2022 (the second period) for the relationship change analysis.

A global oil palm area distribution map, including information on the planted years dataset, was available in Descals et al. (2024) with a spatial resolution of 30 meters. In this study, the map was extracted within the extents of Malaysia and Indonesia and resampled to a resolution of 0.001 degrees using bilinear interpolation (Figure 1).

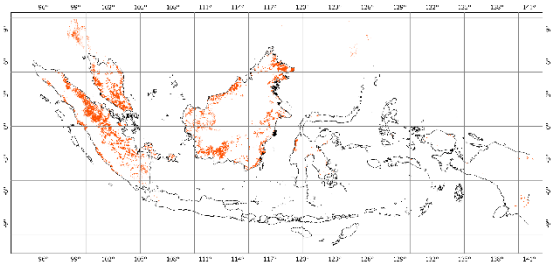

Figure 1. Palm areas in Malaysia and Indonesia in orange color.

Khiabani, et al. (2020) developed a biophysical suitability map for oil palms in Malaysia and parts of Indonesia as of 2017. This study compared identified vulnerable areas with the suitability map to assess any discrepancies between current suitable conditions and potentially vulnerable areas.

2.3 Calibration of the age effect of oil palms

Since oil palms are typically replanted after reaching 20 to 25 years of age, and considering that palms in the immature phase exhibit a higher growth rate compared to mature palms (Foong et al., 2019), the productivity of palms represented by SIF needed to be adjusted for age effects. To calibrate the age effect, this study selected 0.1-degree pixels that matched with pixels of the SIF image and contained an area where palms were planted in 2002 with more than 40% of the grid area. After selecting these pixels, SIF time series data from 2002 to 2022 of these pixels were plotted and a quadratic equation was obtained as a palm growth curve. In the quadratic equation, values from the minimum to the maximum were scaled so that the maximum value was normalized to 1. Then, the inverse of scaled values was calculated to derive weights for each year from planting, thereby calibrating them to the corresponding value at the maximum year. After obtaining age weights, the average planted year was calculated for each 0.1-degree pixel. The average planted year in a grid was determined by multiplying the planted year by its area ratio in a grid and then summing them across the grid. The age weights and average planted year were used to calibrate SIF data at each year. The average planted year was considered as the initial year of growth, and the difference between the year of SIF data and this initial year was considered as the age of the oil palms in the grid. Thus, the age weights were applied to each SIF data based on the identified age so that the SIF data for any year was calibrated to reflect the mature phase. If the planted year was more than 20 years ago, or if a pixel did not contain a palm, a weight of 1 was applied, meaning the original SIF data remained unchanged.

2.4 Calibration of AMSR-E for AMSR2

This study used soil moisture and VOD captured at 6.9 GHz from AMSR-E and AMSR2. However, gaps were observed in two sensors in some pixels. To address this, the median values across all periods for both AMSR-E and AMSR2 were calculated. Then, the ratio of AMSR2 to AMSR-E was determined. This ratio was then used to adjust the AMSR-E data to align it with AMSR2 data.

2.5 Variable relationship analysis

The relationships between SIF and climate or water component variables were calculated as the relationship values to understand the different influences of these variables across the study area. The calculation was based on Seddon et al. (2016), in which the principal component regression (PCR) was employed using monthly time series data of each SIF and variables. In analysis, SIF and each variable were normalized by z-scoring using monthly averages and standard deviation for each month for the first period and the second period at each pixel. Multilinear regression between normalized SIF and scores of each component was performed. The coefficients of significant components ($p<0.1$) were obtained and multiplied by loading values. Lading values represent the correlation coefficient between the original variables and scores of each component, and this process produced the magnitude of the relation between each variable and SIF. The result of positive relationship values indicates a positive correlation between SIF and variables, while negative relationship values mean a negative correlation.

2.6 Variable relationship changes in two periods

Pixels that became more affected by water stress in the second period compared to the first period were identified from the changes in relationship values. For example, if the relationship with precipitation was negative or zero in the first period and then became positive in the second period, this area may indicate increased water stress requiring additional precipitation input, and such pixels and changes in the absolute values of the relationship were extracted. The magnitude of relationship change was determined by calculating the sum of the changes in values across the variables.

2.7 Anomaly of SIF by El Niño from 2015 to 2016

El Niño–Southern Oscillation (ENSO) is a recurrent event of extreme weather. The most severe El Niño hit this region between 2015 to 2016 (Qian et al., 2019). To quantify the impacts of this El Niño on vegetation productivity, the decrease in monthly SIF during the El Niño period compared to the monthly average for each month was calculated. The El Niño event was defined by the Multivariate ENSO Index Version 2 (MEI.v2) (https://psl.noaa.gov/enso/mei/) when the index exceeded 0.5. The deviation for each month during the El Niño period was obtained by subtracting the monthly SIF average during the El Niño from the corresponding monthly average without El Niño. Then, these deviations were summed up for every 3 months. The largest deviation among the 3-month deviations was used as the SIF deviation value.

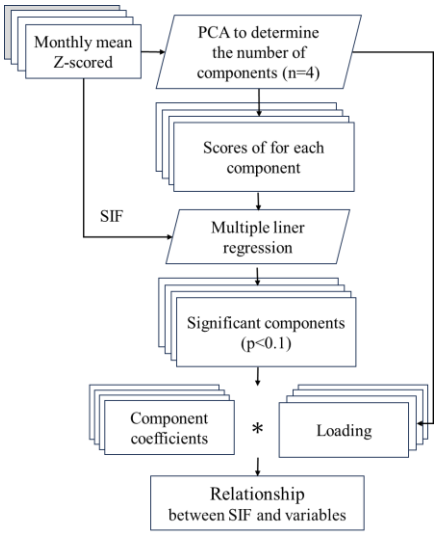

Figure 2. Process flow of relationship analysis

2.8 Comparison with identified vulnerable areas with a biophysical suitable map

Identified vulnerable areas in relationship analysis were visually compared with the biophysical suitable map as of 2017 mentioned in 2.2. To enhance the depiction of the possible vulnerable areas, pixels with 75% percentile of values of relationship change were extracted.

3. Results

3.1 Growth curve for age calibration

The weights of SIF based on age obtained from the palm growth curve (n=10) from 2002 to 2022 are shown in Table 1. The following results used monthly SIF data which had been adjusted with these age weights.

Age	0	1	2	3	4	5	6
weights	1.3	1.3	1.3	1.2	1.2	1.1	1.1
Age	7	8	9	10	11	12	13
weights	1.1	1.1	1.1	1.0	1.0	1.0	1.0
Age	14	15	16	17	18	19	20
weights	1.0	1.0	1.0	1.0	1.0	1.0	1.0

Table 1. Age weights for oil palms

3.2 Variable relationships and their changes in two periods

Figure 3 shows the relationship values between monthly SIF and each variable in the first and second periods. A distinct change can be observed in evaporation in which the positive relationship in the first period decreased to the negative side in the second period, especially in Borneo (Figure 3c). Soil moisture had also clear changes from negative to positive in the whole area of Java Island and the southern area of Borneo (Figure 3d). A similar trend as soil moisture was observed in VOD (Figure 3e). These changes indicated water stress may have occurred requiring moisture in these areas.

3.3 SIF anomaly due to El Niño

Figure 4a shows the spatial distribution of the anomalies of SIF during El Niño from 2015 to 2016 in all study areas, and Figure 4b presents the decreased SIF values among islands where oil palms are currently cultivated. The largest decrease was observed in the entire Java islands with a median of -0.45 W m^{-2} μm^{-1} sr^{-1}, followed by Sulawesi in the southern part with a median of -0.30 W m^{-2} μm^{-1} sr^{-1}. Some islands such as East Malaysia and Sumatra exhibited hotspots of positive anomalies (Figure 4b).

3.4 Relationship changes due to water stress

Fifty-seven percent of pixels where at least one variable changed the relationships due to water stress were identified. This suggested that most areas had water stress. This study focused on pixels where at least one variable was changed as an indicator of water stress.

After identifying sensitive pixels with changing relationships in at least one variable, those pixels were overlaid with pixels where negative anomalies from El Niño occurred. This helped to focus on actual affected areas by extreme climate. Negative relationship changes were scattered, but dense clusters of large changes were notably observed in Java, southern Sulawesi, inland, the east coast and southern Borneo, and the southern part of New Guinea islands. The magnitude of changes in relationship values was highest in Java with a median of 0.44, followed by similar values in other islands. The high relationship change and large SIF anomalies due to El Niño were observed in Java, and relative consistency with such patterns was observed in Sulawesi, Borneo, and New Guinea islands. These matched areas may be considered potentially vulnerable. Whereas, areas with high relationship change and small SIF anomalies may be attributed to their vegetation types (Li et al., 2018).

3.5 Comparison with biophysically suitable map

To enhance the depiction of the possible vulnerable areas identified in relationship change analysis, 75th percentile values of relationship changes were extracted and compared with the biophysical suitability map. The suitable map indicates the east coast of Borneo is less suitable, which was depicted with high relationship change in this study. An interesting finding was that the biophysical suitability map shows relatively high suitability in the southern part of Borneo. However, the relationship analysis in this study indicated vulnerability, as seen in both high and dense changes in relationship values, and SIF anomalies in the same area. Sumatra is also presented as suitable in the suitable map, whereas scattered high relationship changes were observed in this study. Therefore, these regions, especially southern Borneo, may be increasingly vulnerable to climate change impacts.

4. Discussion

4.1 Vegetation response and changes to climate variables

The relationship change analysis revealed more than half of the pixels experienced water stress in the recent period. A distinct change was observed in the relationship change of evaporation where a large decline of its dependency was depicted from the first period to the second period in Malaysia, Borneo, and Sulawesi islands. The finding that soil-related factors were dominant in these regions is partly consistent with reports that tropical regions are less sensitive to precipitation than other factors such as VPD and evapotranspiration (Sun et al., 2016; Oettli et al., 2018; Liu et al., 2020).

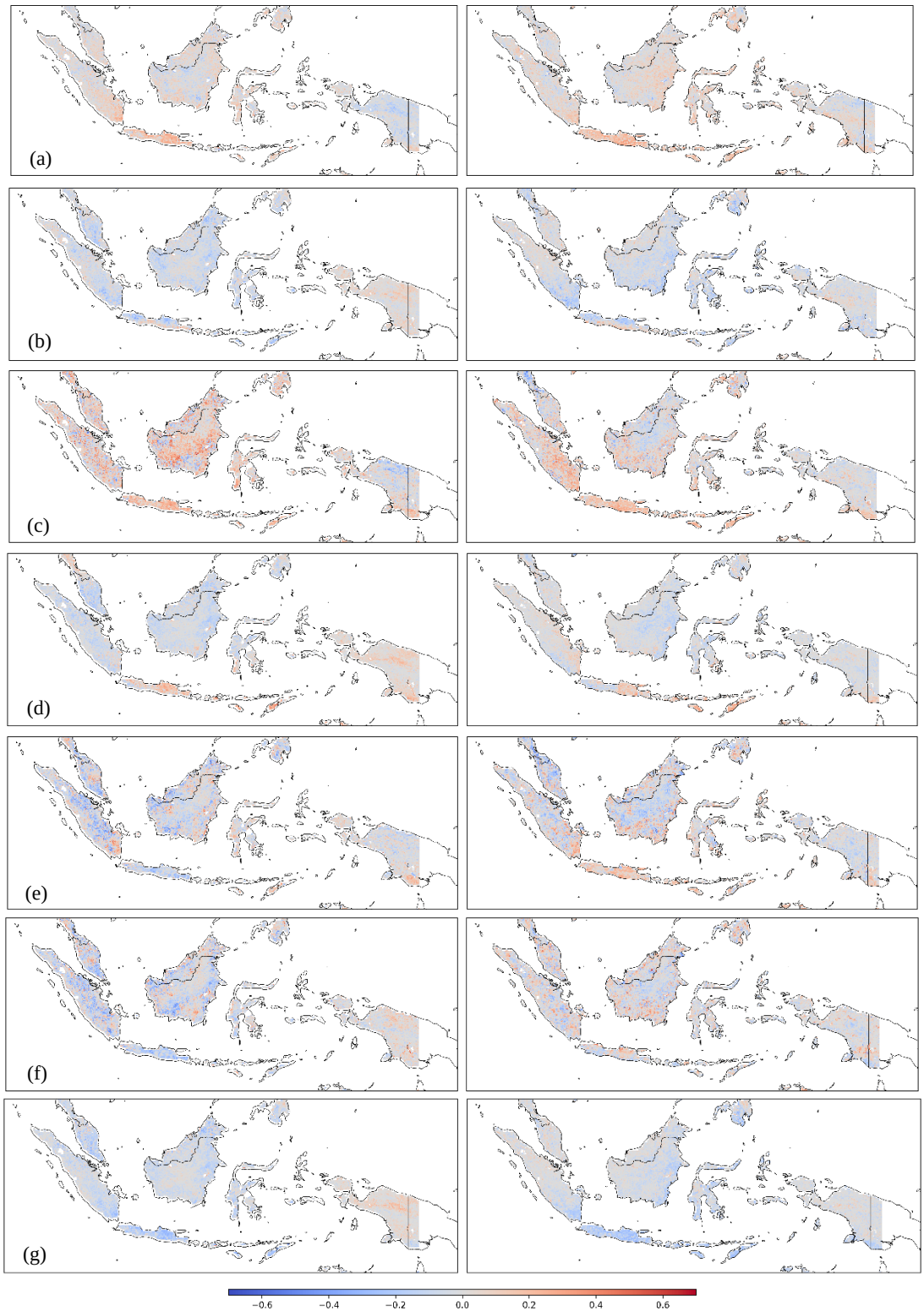

Figure 3. Relationship changes in the first and second periods for (a) precipitation, (b) temperature, (c) evaporation, (d) transpiration, (e) soil moisture, (f) VOD, and (g) VPD. Left column is for 2002-2012 and right column is for 2013-2022. Red color indicates a positive relationship, while blue color indicates a negative relationship.

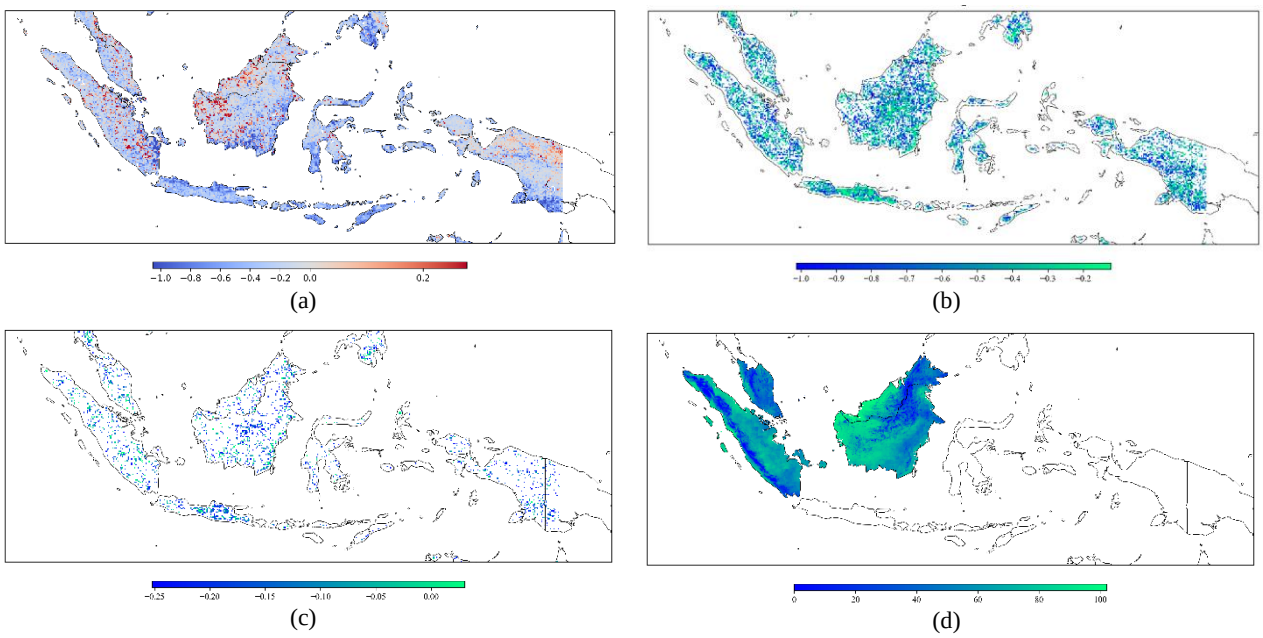

Figure 4. (a) Three months SIF anomalies during El Niño. Blue color indicates a negative anomaly of SIF and red color indicates positive anomaly of in SIF compared to the monthly average. (b) Areas where relationship values of variables were changed due to water-stressed, overlayed by pixels with negative SIF anomalies. Values in the figure are logarithms to base 10 of the sum of changes in the relationship values. (c) Seventy-five percentile of the sum of relationship change values converted to logarithm to base 10, (d) biophysically suitable map (Khiabani et al., 2019) where greater values indicate high suitability for oil palm growth.

4.2 Identification of vulnerable areas to water stress

Relationship analysis indicated possibly vulnerable areas which has high relationship change and negative SIF anomaly during the El Niño in Java, the south and east coast of Borneo, and the southern New Guinea islands. These findings partially agreed with previous studies reporting water stress in these regions (Avia, 2019; Barkey et al., 2019; Tangang et al., 2020).

Whereas regions identified as vulnerable in this study above were also reported by other studies, regions such as Sarawak state in East Malaysia which are also considered to be affected by climate change (Supari et al., 2020) did not decrease SIF during El Niño and had slightly greater relationship change compared. A similar situation was observed in especially inland Borneo. This means West Malaysia, especially Sarawak state and Borneo could maintain vegetation productivity by responding to climate factors. This may be attributed to rich natural forests having different responses from other vegetation types. This finding suggests the great value of natural forests currently withstanding climate disturbances and contributing regional environment.

4.3 Comparison with the biophysical suitability map for oil palm cultivation

The identified possibly vulnerable areas had discrepancies with the biophysical suitable map, especially in the southern part of Borneo where the suitability map indicates suitable while relationship analysis indicated the opposite. Although another study also projected suitable climate conditions in Kalimantan until 2050 (Paterson, 2020), these conditions may not persist as climate change continues to advance.

The findings of this study highlight the heterogeneity and complexity of vegetation responses within the ecosystem. This analysis is crucial for making efficient decisions on implementing adaptation strategies to climate change in palm oil production. It underscores the importance of continuous monitoring of environment, and reflecting it to adaptation actions in vulnerable areas identified by this study, or considering avoidance of further expansion in these areas.

4.4 Limitations and future work

This study did not differentiate land cover or vegetation types in the analysis. Masking land cover with few vegetated areas or differentiating forest and crop areas could provide clearer results for interpretation. In addition, this study utilized monthly SIF and climate datasets at the same temporal timing. However, there would be a time lag for vegetation to respond to climate as reported in several studies (Seddon et al., 2016; Ding et al., 2020). Also, the accumulation effects may exist (Ding et al., 2020). Borth time-lag and accumulation analysis, and adopting corresponding best-fitted temporal datasets are needed. Not only assessing the relationship between the sensitivity of vegetation to climate, but recovery ability is also an important feature for ecosystem to climate resilience (De Keersmaecker et al., 2015).

5. Conclusion

This study analyzed the relationship between monthly SIF and climate variable-related water components in the ecosystem and its change from 2002 to 2012 and from 2013 to 2022 to identify possible vulnerable areas under climate change. Monthly SIF anomaly due to El Niño in 2015 and 2016 and its negative anomalies were also obtained as another indicator of potentially vulnerable areas to extreme weather. The results suggested Java, south part and east coast of Borneo, south Sulawesi, and south

part of New Guinea islands may be vulnerable to climate change. The results partially agreed with climate projections of other studies such as climate impacts in Java and Sulawesi islands. East Malaysia and Borneo were reported to be prone to climate change and El Niño. However, these areas, especially inland Borneo presented a high response to climate but less SIF decline anomaly, which was opposite to other areas. This may be attributed to intact forest. However, recurrent and persistent impacts of climate may hinder vegetation stability. Comparison with the biophysical suitable map and identified vulnerable areas in this study found a relatively similar distribution of vulnerable areas, whereas it revealed discrepancy, especially in the southern part of Borneo island. These findings can contribute to climate adaptation actions.

Acknowledgement

The author expresses gratitude to my professor for supervising this research and provide informative advice to my work.
This study was financially supported by the Foundation for the Promotion of Industrial Science, Japan.

References

Avia, L.Q., 2019. Change in rainfall per-decades over Java Island, Indonesia. *IOP Conf. Ser.: Earth Environ. Sci*. 374, 012037. doi.org/10.1088/1755-1315/374/1/012037

Corley, R.H.V., Tinker, P.B.H., 2015. The Oil Palm. John Wiley & Sons.

De Keersmaecker, W., Lhermitte, S., Tits, L., Honnay, O., Somers, B., Coppin, P., 2015. A model quantifying global vegetation resistance and resilience to short-term climate anomalies and their relationship with vegetation cover. *Global Ecol. Biogeogr*. 24, 539–548. doi.org/10.1111/geb.12279

Descals, A., Gaveau, D.L.A., Wich, S., Szantoi, Z., Meijaard, E., 2024. Global mapping of oil palm planting year from 1990 to 2021. *Earth Syst. Sci. Data Discuss*. 1–24. doi.org/10.5194/essd-2024-157

Ding, Y., Li, Z., Peng, S., 2020. Global analysis of time-lag and -accumulation effects of climate on vegetation growth. *Int J. appl. Earth Obs*. 92, 102179. doi.org/10.1016/j.jag.2020.102179

Foong, S.Z.Y., Goh, C.K.M., Supramaniam, C.V., Ng, D.K.S., 2019. Input–output optimisation model for sustainable oil palm plantation development. *Sustainable Production and Consumption* 17, 31–46. doi.org/10.1016/j.spc.2018.08.010

Li, D., Wu, S., Liu, L., Zhang, Y., Li, S., 2018. Vulnerability of the global terrestrial ecosystems to climate change. *Glob. Change Biol*. 24, 4095–4106. doi.org/10.1111/gcb.14327

Li, X., Xiao, J., 2019. A Global, 0.05-Degree Product of Solar-Induced Chlorophyll Fluorescence Derived from OCO-2, MODIS, and Reanalysis Data. *Remote Sensing* 11, 517. doi.org/10.3390/rs11050517

Liu, Y., Wang, Y., Yang, Y., Jiang, H., Jing, W., 2024. Impacts of hydrometeorological controls on vegetation productivity: Evidence from satellite observations and reanalysis. *Ecol. Indic*. 161, 111976. doi.org/10.1016/j.ecolind.2024.111976

Loh, J.L., Tangang, F., Juneng, L., Hein, D., Lee, D.-I., 2016. Projected rainfall and temperature changes over Malaysia at the end of the 21st century based on PRECIS modelling system. *Asia-Pacific J Atmos Sci* 52, 191–208. doi.org/10.1007/s13143-016-0019-7

Moron, V., Robertson, A.W., Qian, J.-H., 2010. Local versus regional-scale characteristics of monsoon onset and post-onset rainfall over Indonesia. *Clim Dyn* 34, 281–299. doi.org/10.1007/s00382-009-0547-2

Oettli, P., Behera, S.K., Yamagata, T., 2018. Climate Based Predictability of Oil Palm Tree Yield in Malaysia. *Sci. Rep*. 8, 2271. doi.org/10.1038/s41598-018-20298-0

Paterson, R.R.M., 2020. Oil palm survival under climate change in Kalimantan and alternative SE Asian palm oil countries with future basal stem rot assessments. *Forest Pathology* 50, e12604. doi.org/10.1111/efp.12604

Qian, X., Qiu, B., Zhang, Y., 2019. Widespread Decline in Vegetation Photosynthesis in Southeast Asia Due to the Prolonged Drought During the 2015/2016 El Niño. *Remote Sensing* 11, 910. doi.org/10.3390/rs11080910

Seddon, A.W.R., Macias-Fauria, M., Long, P.R., Benz, D., Willis, K.J., 2016. Sensitivity of global terrestrial ecosystems to climate variability. *Nature* 531, 229–232. doi.org/10.1038/nature16986

Supari, Tangang, F., Juneng, L., Cruz, F., Chung, J.X., Ngai, S.T., Salimun, E., Mohd, M.S.F., Santisirisomboon, J., Singhruck, P., PhanVan, T., Ngo-Duc, T., Narisma, G., Aldrian, E., Gunawan, D., Sopaheluwakan, A., 2020. Multi-model projections of precipitation extremes in Southeast Asia based on CORDEX-Southeast Asia simulations. *Environ. Res*. 184, 109350. doi.org/10.1016/j.envres.2020.109350

Tang, A.C.I., Melling, L., Stoy, P.C., Musin, K.K., Aeries, E.B., Waili, J.W., Shimizu, M., Poulter, B., Hirata, R., 2020. A Bornean peat swamp forest is a net source of carbon dioxide to the atmosphere. *Glob. Change Biol*. 26, 6931–6944. doi.org/10.1111/gcb.15332

Tangang, F., Chung, J.X., Juneng, L., Supari, Salimun, E., Ngai, S.T., Jamaluddin, A.F., Mohd, M.S.F., Cruz, F., Narisma, G., Santisirisomboon, J., Ngo-Duc, T., Van Tan, P., Singhruck, P., Gunawan, D., Aldrian, E., Sopaheluwakan, A., Grigory, N., Remedio, A.R.C., Sein, D.V., Hein-Griggs, D., McGregor, J.L., Yang, H., Sasaki, H., Kumar, P. 2020. Projected future changes in rainfall in Southeast Asia based on CORDEX–SEA multi-model simulations. *Clim Dyn* 55, 1247–1267. doi.org/10.1007/s00382-020-05322-2